Mutational Analysis of the Catalytic Residues Lysine 230 and Tyrosine 160 in the NADP$^+$-Dependent Isocitrate Dehydrogenase from *Escherichia coli*†

Myoung E. Lee,‡,§ David H. Dyer,|| Ophir D. Klein,§ Jill M. Bolduc,|| Barry L. Stoddard,|| and D. E. Koshland, Jr.*,§

Center for Advanced Materials, Lawrence Berkeley Laboratory, and Department of Molecular and Cell Biology, University of California, Berkeley, California 94720, and Fred Hutchinson Cancer Center, Division of Basic Sciences, Program Structural Biology, 1124 Columbia Street, Seattle, Washington 98104

Received July 18, 1994; Revised Manuscript Received October 10, 1994⊗

ABSTRACT: Two site-directed mutants of isocitrate dehydrogenase (IDH) of *Escherichia coli* have been studied by site-directed mutagenesis kinetic and structural studies. Substitution of phenylalanine for tyrosine at position 160 (Y160F) showed 0.4% of the k_{cat} of wild-type with isocitrate as substrate, while the K_m for isocitrate remained unchanged. When the postulated intermediate, oxalosuccinate, was enzymatically decarboxylated, Y160F showed a higher k_{cat} and a similar K_m to the wild type values. The rate of reduction of oxalosuccinate to isocitrate by the Y160F mutant was greatly decreased relative to the wild-type. Substitution of methionine for lysine at position 230 decreased k_{cat} to 1.1% of that of the wild-type and K_m increased by a factor of 500−600. The decarboxylation of oxalosuccinate was undetectable for the K230M mutant. The structure of the site-directed mutants of IDH with and without a bound complex of isocitrate and Mg^{2+} was solved at 2.5 Å resolution and compared by difference mapping against previously determined enzyme structures. The structural studies show that (i) the overall protein-folding side chain conformations and active sites of both mutants are isomorphous with wild-type enzyme, (ii) isocitrate and magnesium bind to both enzyme mutants with the same relative conformation and binding interactions as wild-type enzyme, and (iii) the mutated side chains (Phe 160 and Met 230) are positioned for catalysis in a similar conformation as that observed for the wild-type enzyme. Hence, the alteration of the side chain functional groups is directly related to the loss of enzyme activity. Possible roles of the active site tyrosine and lysine are discussed.

Isocitrate dehydrogenase (IDH)[1] [D$_s$-*threo*-isocitrateNAD(P)$^+$ oxidoreductase (decarboxylating), EC 1.1.1.42] is a key enzyme in the Krebs cycle in eukaryotic systems and occupies a branch point between the Krebs cycle and the glyoxylate shunt in bacterial and plant systems. The mammalian enzyme (Atkinson & Koshland, 1977) is regulated allosterically, but the bacterial enzyme appears to be regulated largely by phosphorylation, with an increase of the K_m values for isocitrate of phosphorylated enzyme relative to dephosphorylated enzyme (Dean & Koshland, 1990).

Sequence homologies between the bacterial enzyme and the eukaryotic enzymes are significant. For example, NADP isocitrate dehydrogenases from *Escherichia coli* and *Saccharomyces cerevesiae* share 33% sequence identity (Haselbeck & McAlister-Henn, 1991a,b; Haselbeck *et al.*, 1992; Cupp & McAlister-Henn, 1992), but the bacterial enzyme is known to lack a "Rossman fold" often found in many of the eukaryotic dehydrogenase systems (Hurley *et al.*, 1989, 1990b). Moreover, pioneering isotopic studies on mechanisms have been reported by Grissom and Cleland (1988).

Hurley *et al.* (1991) reported from the structure of isocitrate-bound IDH that two residues appear to be positioned as possible catalytic acids, lysine 230 and tyrosine 160. The distance between the β-carboxyl oxygen of isocitrate and the hydroxyl oxygen of tyrosine 160 is 2.8 Å, while the distance to the nitrogen of the side chain of lysine 230 is 3.0 Å (Hurley *et al.*, 1991). According to the stereochemistry of the reaction which shows that protonation of the β-carbon takes place with retention of configuration (Lienhard & Rose, 1964), tyrosine 160 and lysine 230 are good candidates for essential catalytic residues in decarboxylation, since they are facing the leaving β-carboxylate. The X-ray structure of isopropylmalate dehydrogenase from *Thermus thermophilus* HB8 was reported (Imada *et al.*, 1991), and there is a strong similarity in the folding topology between IMDH and IDH as suspected from the sequence homology. In isopropylmalate dehydrogenase, tyrosine 139, which is similar to tyrosine 160 in isocitrate dehydrogenase, has been changed to a phenylalanine with approximately a 2-fold change in K_m for isopropylmalate and a 14-fold improvement in affinity for NAD$^+$ (Miyazaka & Oshima, 1993).

Tyrosine 160 and lysine 230 have their analogs in the conserved region of the NADP$^+$-dependent IDH1 from yeast, NAD$^+$-dependent IDH2 from yeast, and NADP$^+$-dependent IDH from pig mitochondria (Haselbeck & McAlister-Henn, 1991a,b; Haselbeck *et al.*, 1992). The only exception is NAD$^+$-dependent IDH1 from yeast mitochondria which has phenylalanine instead of tyrosine at position 147 (equivalent to position 160 in IDH from *E. coli*) (Cupp & McAlister-Henn, 1992).

In this study we have mutated lysine 230 and tyrosine 160 to methionine and phenylalanine, respectively, to study their

† Support was obtained from the Center for Advanced Materials, Lawrence Berkeley Laboratory, for D.E.K. and M.E.L. and from NIH Grant R01-GM49857 for B.S.

‡ Center for Advanced Materials, Lawrence Berkeley Laboratory, University of California.

§ Department of Molecular and Cell Biology, University of California.

|| Program Structural Biology.

⊗ Abstract published in *Advance ACS Abstracts,* December 15, 1994.

[1] Abbreviations: IDH, isocitrate dehydrogenase; D-isocitrate, D$_s$-*threo*-isocitrate; α-KG, α-ketoglutarate; OSA, oxalosuccinate.

0006-2960/95/0434-378$09.00/0

roles in catalysis using both the substrate isocitrate and the postulated intermediate oxalosuccinate. We have also determined the X-ray structures of these mutants in the presence and absence of bound isocitrate and magnesium to further strengthen our identification of their roles.

EXPERIMENTAL METHODS

Kinetic Procedures. Plasmid pTK513, which carries the *icd* gene *E. coli* in a pEMBL vector (Dente *et al.*, 1983), was used for mutagenesis as well as overproduction of IDH. Oligonucleotide-directed mutagenesis was done using a uracil-labeled single-stranded template as described in Kunkel (1985). The plasmid-containing mutated sequence of IDH was sequenced to verify the identity of the mutants.

Mutant IDH's were overproduced in an IDH-free *E. coli* strain, JLK1, which has a deletion in *icd*. Enzymes were purified as described in Garnak and Reeves (1979) with modification in the last step, in which the enzyme was eluted from a Affi-Gel blue column (Bio-Rad) with a step gradient of 0.5 M NaCl instead of a solution of NADP (Dean *et al.*, 1989). Homogeneity of the protein was determined by SDS−polyacrylamide gel electrophoresis. Purified proteins were stored at −80 °C. Protein concentrations were determined by the absorbance at 280 nm using a molar extinction coefficient for IDH of 66 700 M^{-1} cm^{-1}. (2*R*,3*S*)-Isocitrate, D- and L-α-hydroxyglutarate, barium oxalosuccinate, and NADP(H) were purchased from Sigma. Potassium oxalosuccinate was prepared from barium salt according to Ochoa (1948). The concentrations of α-KG and OSA were measured enzymatically as described in Grissom and Cleland (1988).

The steady state kinetics were done using a saturating concentration of one substrate and varying the other substrate concentration. The rates of oxidative decarboxylation of isocitrate in the presence of NADP were measured by spectrophotometrically monitoring the change in the absorbance of NADPH at 340 nm using a molar extinction coefficient of 6220 M^{-1} cm^{-1} on a Hewlett-Packard 8452A spectrophotometer. The rates of reduction of oxalosuccinate in the presence of NADPH were determined in a similar fashion by measuring the disappearance of NADPH at 340 nm. The disappearance of OSA was measured spectrophotometrically at 240 nm (Ochoa, 1948) at pH 7.8 in Tris/HCl to determine the decarboxylation reaction rates. The molar extinction coefficient for the decarboxylation of OSA ($\epsilon_{240,OSA} - \epsilon_{240,\alpha\text{-KG}}$) under this condition was 498 M^{-1} cm^{-1}. The nonenzymatic decarboxylation rates were subtracted from the overall rates. The percentage error in measuring the nonenzymatic decarboxylation was 5.6% under this condition. To prevent α-ketoglutarate from interfering with the assays, glutamate-pyruvate transaminase was added to the assay mixture to remove α-ketoglutarate. Similar kinetic values were observed whether this treatment was used or not, probably due to the very low affinity of α-ketoglutarate compared to oxalosuccinate.

Crystallographic Procedures. Isocitrate dehydrogenase was purified (Reeves *et al.*, 1972; LaPorte *et al.*, 1985) and crystallized (Hurley *et al.*, 1989) as described previously. Protein at 60 mg/mL was diluted with d/d H_2O to a final concentration of 20 mg/mL. Hanging drop crystallizations were set up at room temperature, and crystals grew within a month which were 0.5−1.0 mm per side, space group $P4_32_12$. The unit cell dimensions of both mutants in the presence and absence of bound substrate consistently refined to values within 0.5% of the previously published dimensions for the wild-type enzyme during data processing (Table 1).

The crystals were transferred to a 1 mL volume of artificial mother liquor (generally 10% higher ammonium sulfate than that used to grow the crystals) and either used directly in data collection or soaked with isocitrate and magnesium; 100 μL of 10× stock solution (1 M isocitrate and Mg^{2+}) was added directly to the buffer containing the crystals, and the soak proceeded overnight. The crystals were then mounted in quartz capillaries with mother liquor at either end of the capillary. The mount was sealed with mineral oil and paraffin wax.

Data were collected on an *R*-axis imaging plate area detector with Rigaku RU-200 rotating anode X-ray generator operating at 50 kV, 80 mA. Operating a reduced current was helpful for maintaining crystal stability in the beam. For all four data sets (apoenzyme and substrate-bound form of each mutant), two crystals were used to collect a data set to 2.5 Å resolution using 15° rotations at 30 min/deg. We applied a 2.0 σ cutoff followed by rejection of all reflections with structure factor amplitudes less than one-third the average value of *F* for the overall data set (approximately 5% of the total reflections processed). For all data sets, over 80% of the unique data was present in the final data set. The internal merging R_{symm} for each crystal and overall R_{merge} between crystals for each individual data set are shown in Table 1 and compare favorably with past reported IDH structure determinations (Hurley *et al.*, 1989, 1990a,b, 1991; Stoddard *et al.*, 1993a,b). The *R*-axis data collection software package (Molecular Structure Corp.) was used to collect and process the data, and protein difference Fourier maps were calculated using the software package PROTSYS. The results of data processing and refinement statistics are given in Table 1.

In order to assess the structural effect of the side-directed mutations on the structure of the enzyme active site, F_o(apoenzyme, mutant) − F_o(apoenzyme, wild-type) difference Fourier syntheses were calculated for each mutant using the experimentally determined structure factor amplitudes for the mutant and the wild-type apoenzymes and phases calculated from wild-type enzyme coordinates from the Brookhaven Protein Data Bank (Bernstein *et al.*, 1977) as the initial model (Hurley *et al.*, 1989; accession number 3ICD). These maps were examined using the program QUANTA (Molecular Simulations) on a Silicon Graphics Indigo workstation. The data sets were placed independently into an XPLOR-simulated annealing refinement (Brunger *et al.*, 1987) using the structure of uncomplexed isocitrate dehydrogenase (with the appropriate mutation) as the initial model. XPLOR refinement was performed against the data set from 50 to 2.5 Å resolution. We used protocol in which the structure, after the initial static energy minimization, is heated to 4000 °C and then immediately placed into a slow cooling (50 ps) annealing minimization. No extended dynamics were performed during the heat stage of the refinement. Sequential cycles of least squares refinement were run using the same initial model. The structures were examined for changes due to the presence of the mutations, and then the refinements were continued after incorporation of solvent molecules.

Table 1: Data Processing and Refinement Statistics

	Y160F	Y160F + substrate	K230M apo	K230M + substrate
no. of crystals	2	1	2	2
exposure time (min/deg)	30	30	30	30
rotations ($\Delta\Phi$, total frames)	2°, 25	2°, 25	2°, 25	2°, 25
total unique reflections	22143	20959	24707	23643
	Final Data Set and Refinement			
R_{merge}[a]	0.090		0.095	0.083
R_{symm}[b]	0.064	0.061	0.066	0.058
resolution (Å)	2.5	2.5	2.5	2.5
refinement R-factor[c]	0.215	0.205	0.223	0.197
	Structural Statistics			
bond distance rms (Å)	0.021	0.019	0.023	0.023
bond angle rms (deg)	3.56	3.44	4.01	3.69
dihedral angle rms (deg)	24.90	25.31	25.69	25.47

[a] Overall R-factor (on intensities) between the same reflections from each crystal after scaling, correction for absorption and polarization. $R = \sum_j(I_1(j) - I_2(j))/\sum_j(I(j))$. [b] Initial overall R-factor (on intensities) between all symmetry-related reflections in the final merged data set. [c] $R = \sum_j|(F_{obs}(j) - F_{calc}(j))|/\sum_j(F_{obs}(j))$.

F_o(isocitrate, Mg^{2+}) − F_o(apoenzyme) difference Fourier syntheses were then calculated for each mutant using the experimentally determined structure factor amplitudes in the presence and absence of bound substrate and initial phases calculated with the coordinates of wild-type apoenzyme (from the Brookhaven Protein Data Bank as described above) in order to determine the structure of the substrate-bound enzyme complex for each mutant. These maps were examined as before. Isocitrate and magnesium were manually built into the structure, and the refinement was continued using XPLOR. No heating and annealing were performed in the second round of refinement. The occupancy of the bound substrate and metal was fixed at unity during the refinement, and their individual atomic temperature factors were allowed to refine independently. The values of these B-factors ranged from 20 to 30 $Å^2$ and are comparable to the surrounding protein side chains in the active site, indicating that the assignment of the bound ternary complex is correct. The results of the final refinement are shown in Table 1.

RESULTS

Structure of the IDH Y160F Site-Directed Mutant. The effect of removing the phenolic hydroxyl from tyrosine 160 in the enzyme active site is small but easily observable (Figure 1). The position of the aromatic ring of phenylalanine 160 is found to be almost identical to tyrosine 160 in the wild-type enzyme. However, the loss of this hydrogen-donor group causes a motion of two adjoining side chains toward the phenylalanine ring: the arginine 119 side chain moves toward the vacated hole in the protein structure by approximately 2 Å, and the side chain of arginine 129 moves toward the same position by 1.2 Å. A third active site arginine moves by a smaller amount in the same direction. These movements are accomplished primarily through bond rotations along the arginine side chains; their respective backbone segments move by less than 0.5 Å. The net result of these rearrangements is to replace the side chain volume and the hydrogen-bonding potential of the mutated tyrosine residue, which in the absence of bound substrate is associated with a loosely bound solvent molecule; these interactions are replaced by the arginine residues noted above.

Difference maps of the mutant enzyme in the presence of bound isocitrate clearly indicate that the metal/substrate chelate binds in the same relative position and orientation as in the wild-type enzyme. The largest difference is in the bound metal, which is displaced by slightly less than 0.5 Å from the magnesium position in the wild-type structure. The metal is easily modeled in the strongest peak in the F_o(substrate) − F_o(apoenzyme) difference map of the site-directed mutant (Figure 1). The bound isocitrate is located in the same position and orientation as in the wild-type complex, except for a small rigid-body rotation of approximately 8° which allows the isocitrate to maintain proper bonding geometry to the metal. The mutant enzyme/substrate complex and the specific interactions between substrate and the active site side chains are isomorphous with the wild-type enzyme/substrate complex; the mutant phenylalanine side chain is located in the same position as the original wild-type tyrosine. With the exception of the missing hydroxyl group, the substrate complex appears to be catalytically competent when compared to the wild-type enzyme/isocitrate−magnesium structure, at least with respect to interactions between bound substrate and the enzyme site.

Structure of the IDM K230M Site-Directed Mutant. The net structural change caused by replacing the five-atom primary amino group side chain of lysine 230 with the four-atom thiol ether of methionine is smaller than the tyrosine to phenylalanine mutation described above (Figure 2). The largest movement in the active site is a rotation of the torsion angle between the Cα and Cβ atoms of serine 113 by approximately 30°, resulting in a movement of the γ-hydroxyl by 1 Å. A pair of side chains which form weak polar interaction with the wild-type lysine side chain amino group, aspartate 283′ and asparagine 232′, rotates slightly away from the methionine residue by approximately 0.5 Å. All other active site residues and their side chains are completely isomorphous with the wild-type apoenzyme. Distal to the active site, threonine 104 (a residue located at the dimer interface 14 Å from the isocitrate binding site) shifts by 1.5 Å; this is the only other significant motion produced by the mutation of lysine 230. Since residue 230 is involved in stabilization of the dimer interface and contributes to the active site binding of isocitrate between subunits, the movement of this threonine could be the result of the propagation of small structural changes along the dimer interface.

The difference map of the K230M in the presence and absence of bound isocitrate and magnesium (Figure 2) shows that the substrate and metal are bound in an identical position and conformation as in the wild-type enzyme. The side chain of lysine 230 extends approximately 1 Å further toward the bound isocitrate than the methionine residue, indicative of both the extra atom in the lysine side chain and the formation of a specific polar binding interaction with the carboxyl of isocitrate in the wild-type enzyme/substrate complex. The other members of the catalytic site are unchanged relative to the wild-type enzyme/substrate complex. As in the case of Y160F, the substrate and the surrounding residues are

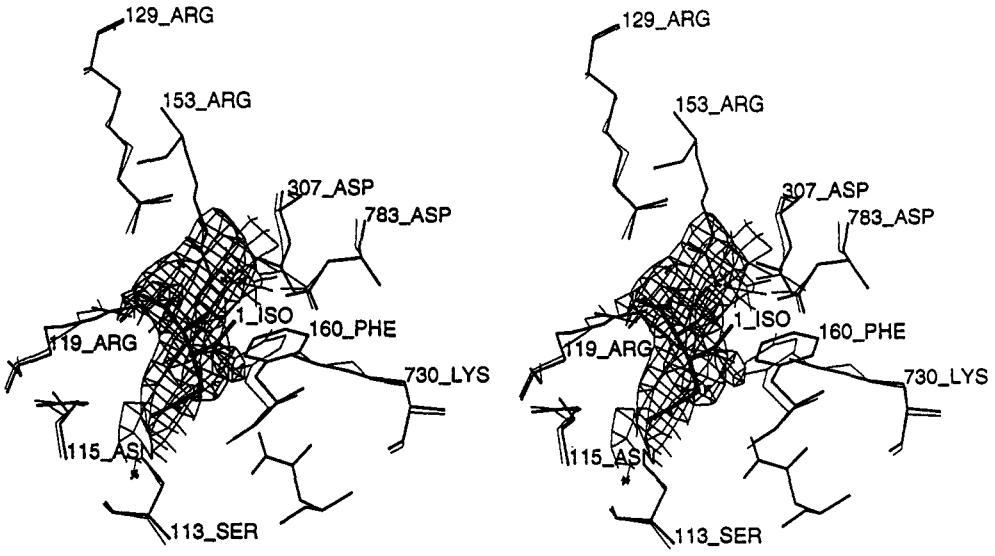

FIGURE 1: $[F_o(\text{isocitrate, } Mg^{2+}) - F_o(\text{apoenzyme})]^{\alpha}$ calculated difference Fourier map calculated for the tyrosine 160 to phenylalanine site-specific mutant. The map was calculated with the experimentally determined structure factor amplitudes in the presence and absence of bound substrate, and initial phases were calculated with the coordinates of wild-type apoenzyme (from the Brookhaven Protein Data Bank) in order to determine the unbiased structure of the substrate-bound enzyme complex for each mutant. The density shown modeled by isocitrate (thickest bonds) and magnesium (dark sphere) is the strongest feature in the map. The mutant active site residues are shown as thick bonds, and the wild-type active site residues from the isocitrate/magnesium complex (Hurley *et al.*, 1990a) are shown as light bonds. The mutated residue is labeled at 160 PHE.

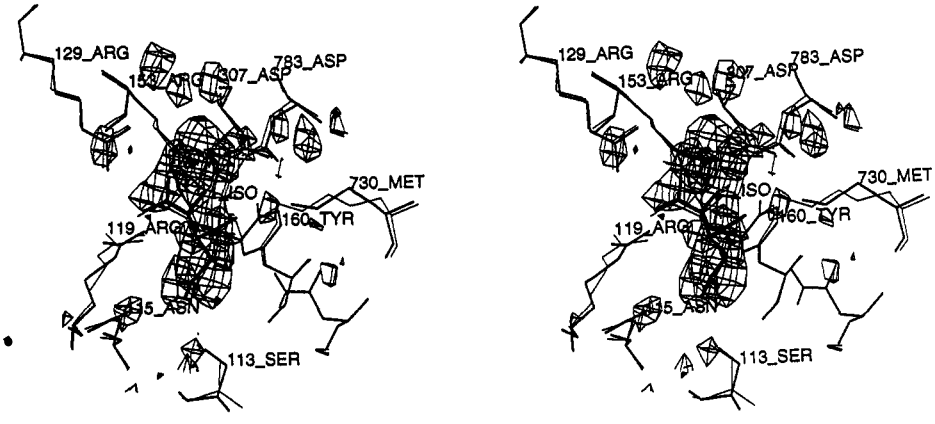

FIGURE 2: $[F_o(\text{isocitrate, } Mg^{2+}) - F_o(\text{apoenzyme})]^{\alpha}$ calculated difference Fourier map calculated for the lysine 230 to methionine site-specific mutant. The map was calculated with the experimentally determined structure factor amplitudes in the presence and absence of bound substrate, and initial phases were calculated with the coordinates of wild-type apoenzyme (from the Brookhaven Protein Data Bank) in order to determine the unbiased structure of the substrate-bound enzyme complex for each mutant. The density shown modeled by isocitrate (thickest bonds) and magnesium (dark sphere) is the strongest feature in the map. The mutant active site residues are shown as thick bonds, and the wild-type active site residues from the isocitrate/magnesium complex (Hurley *et al.*, 1990a) are shown as light bonds. The mutated residue is labeled as 730 MET.

positioned appropriately for catalysis and proton transfer (relative to the known productive complex structure of the wild-type enzyme), leading to the conclusion that the reduction of the individual rate constants for these mutations is indicative of the loss of a specific chemical group in the active site rather than an indirect structural effect leading to unproductive binding ot substrate.

Kinetics of the Y160F Mutant. The reaction catalyzed by IDH consists of two distinct reactions which are readily separable: dehydrogenation of isocitrate (a step which involves deprotonation of the hydroxyl group and transfer of a hydride from the C2 carbon of isocitrate) followed by elimination of the β-carboxyl group and formation of α-ketoglutarate (which also involves specific proton transfer by the enzyme). The putative intermediate which separates these reactions steps is oxalosuccinate. By mutagenizing a pair of residues which are positioned appropriately for facilitating the dehydrogenation and elimination steps, we hope to expand our understanding of the enzyme mechanism and facilitate direct structural studies of productive enzyme intermediates using Laue crystallography. For both mutants, as well as wild-type enzyme, we can directly measure the overall rates in both directions, as well as the rates of individual half-reactions using oxalosuccinate as substrate.

The results of the kinetic analysis of the K230M and Y160F mutants are shown in Table 2. The Y160F mutation causes a decrease in k_{cat} of isocitrate to about 1/200 of its wild-type value, and the K_m decreases by about 10%. The rate of decarboxylation of oxalosuccinate by this mutant actually increases by a factor of 1.8 (k_{cat} mutant/k_{cat} wt = 1.8), whereas the K_m of this step increases by about 67%. Thus in this case, the k_{cat}/K_m decreases by 76%. The rate of reduction of the oxalosuccinate to isocitrate by this mutant decreases by a factor of 1/50, about 50-fold. Hence it

Table 2: Kinetic Constants of IDH's in Various Reactions

reactions	kinetic constants	enzymes		
		WT	K230M	Y160F
D-isocitrate to α-KG	K_{cat} (s^{-1})	76.2	0.850	0.311
	K_m (M)	0.0000114	0.00603	0.0000096
	k_{cat}/K_m (s^{-1} M^{-1})	6710000	141	32300
	k_{cat}/K_m, norm	1	0.0000210	0.00481
OSA to D-isocitrate (at pH 708)	K_{cat} (s^{-1})	1.41	0.368	0.053
	K_m (M)	0.00034	0.002	0.000562
	K_{cat}/K_m (s^{-1} M^{-1})	4150	184	94.3
	K_{cat}/K_m, norm	1	0.0443	0.0227
OSA to α-KG (at pH 7.8)	K_{cat} (s^{-1})	20.6	undetectable	36.2
	K_m (M)	0.00022	undetectable	0.00022
	K_{cat}/K_m (s^{-1} M^{-1})	93600	undetectable	165000
	K_{cat}/K_m, norm	1	undetectable	1.76
D-α-hydroxyglutarate to α-KG (at pH 7.8)	K_{cat} (s^{-1})	0.000724	0.000213	0.00067
	K_m (M)	0.003	0.0129	0.0106
	K_{cat}/K_m (s^{-1} M^{-1})	0.241	0.0165	0.0632
	K_{cat}/K_m, norm	1	0.0685	0.262

appears that tyrosine 160 participates in the hydride transfer step and has little or no role in the normal decarboxylation step, other the binding interactions to the substrate, intermediate, and product species.

Kinetics of the K230M Mutant. The replacement of the lysine at position 230 reduces k_{cat} for isocitrate by about 1/60 of the wild-type value and increases the K_m by a factor of 500. The decarboxylation of oxalosuccinate to α-ketoglutarate is undetectable in the K230M mutant relative to the nonenzymatic decarboxylation rate (which is substantial), emphasizing the crucial role of the lysine in the decarboxylation step when the intermediate is complexed to the enzyme active site. Obviously the positively changed lysine which is juxtaposed to the β-carboxyl of isocitrate plays a vital role in binding and catalysis. It is perfectly positioned to assist in the decarboxylation and to donate a proton to the resulting carbanion. Lienhard and Rose (1994) have shown that an H^+ replaces the carboxyl with retention of configuration, and the lysine and tyrosine are both appropriately positioned for this role.

The rate of reduction of the oxalosuccinate to isocitrate is reduced by a factor of 4, and the K_m is increased by a factor of 6, indicating that the lysine plays a less important role in the hydride transfer but obviously supplies some force of attraction and/or perhaps helps orient the substrate in the step.

Kinetics of α-Hydroxyglutarate. α-Ketoglutarate has been reported to be reduced to α-hydroxyglutarate by pig heart NADP-dependent IDH from ^{13}C-NMR studies (Erlich & Colman, 1987). We report the D-isomer of α-hydroxyglutarate which lacks the β-carboxylate of isocitrate is a substrate for the wild-type *E. coli* IDH and for the K230M and Y160F mutants.

The α-hydroxyglutarate is far less good as a substrate than isocitrate, but it tends to be consistent with the above conclusions. It lacks the β-carboxyl group so it should show much less affinity to the wild-type. The deletion of lysine 230 should have little or no effect on this rate since the β-carboxyl has been removed. Both are observed to be true.

DISCUSSION

In the foregoing description, two residues, tyrosine 160 and lysine 230, have been modified with no effect on the folding of the protein to a wild-type structure and little change in conformation of the active site and binding of substrate. Therefore, the changes that occur in the kinetic profile of these enzyme mutants must be caused by a combination of two possible effects: (i) alteration of the catalytic activity of the enzyme caused by the specific alteration of the side chain chemistry and/or (ii) structural differences in the productive ternary complex of enzyme, substrate, and cofactor formed during turnover which are not revealed in the binary complexes reported here. As discussed below, the kinetic and structural information available for this enzyme indicates that the primary effect of these site-directed mutations is to reduce specific rate constants at separate stages of catalysis. This occurs primarily by affecting the ability of the enzyme to catalyze specific reaction steps such as deprotonation of the isocitrate molecule and elimination of the β-carboxyl.

The change of the tyrosine 160 to a phenylalanine 160 actually improves the binding of the substrate, isocitrate, slightly but decreases the catalytic rate by a factor of about 1/250. The change of the lysine 230 to methonine decreases the catalytic rate by a factor of a little less than 100 but increases the K_m by a factor of over 500, a major decrease in the binding affinity. Essentially no change in the structure of the enzyme is observed in either case, and the only difference in protein is the change in atoms between lysine and methonine and between tyrosine and phenylalanine. Thus, it is clear that the reason for the activity changes lies in the change in chemistry and not the folding of the protein nor the conformation at the active site. The minor effect of the K230M mutation on the overall rate is at first surprising but can be understood if we consider a back-up role for the tyrosine 160 residue. The rate of the overall reaction drops by only a factor of 100 in the K230M mutation, a smaller factor than might be expected if the lysine 230 is the key proton donor in the decarboxylation. However, the tyrosine 160 is situated near the lysine 230 in the three-dimensional space and may play the role of a proton donor in the absence of K230.

These results (typical of mutagenesis studies in many proteins) provide information interesting in themselves but much more so when the kinetics of the postulated intermediate oxalosuccinate (OSA) are examined. In this case the mutations have effects which help define the system. The absence of lysine 230 stops the OSA to α-ketoglutarate reaction completely, whereas the Y160F mutation has

essentially no effect on this reaction. Thus lysine must play a vital role in the decarboxylation step, whereas tyrosine 160 plays little or no role. The OSA to isocitrate reaction on the other hand is decreased by a factor of 4 by loss of lysine 230, and the binding affinity is decreased by a factor of 6, an important but far less crucial role. The Y160F change, however, has a strong effect (30-fold) on the hydrogenation step, a result consistent with the conclusion that its role as wild-type is mainly in the dehydrogenation step. These conclusions for isocitrate dehydrogenase are particularly interesting, since Migazaki and Oshima (1993a) have shown that tyrosine 139 and lysine 183 are present in all isopropylmalate dehydrogenase found so far and that a tyrosine to phenylalanine mutation at residue 139 causes a 16-fold decrease in k_{cat}.

The α-hydroxyglutarate results also reinforce these conclusions since there is no decarboxylation reaction with this substrate. The k_{cat} remains constant in the Y160F mutant, and the K_m changes to lower affinity by a factor of 3. The K230M mutant loses a factor of 3 in k_{cat} and factor of about 4 in binding affinity. The absence of the β-carboxyl group in the hydroxyglutarate has a dramatic effect on the overall velocity but seems to confirm the role of the lysine 230 reached in studies with isocitrate.

Isocitrate dehydrogenase of *E. coli* is emerging as an enzyme in which definitive structure function studies can be performed. Already sequence homologies in other isocitrate dehydrogenases in pig heart (Hasselbeck *et al.*, 1992) and yeast (Hasselbeck & McAlister, 1991a) are leading to suggestions of similar amino acid residue functions in these other enzymes at their active sites. The fact that some of these enzymes use NAD instead of NADP does not change the basic mechanism and therefore provides an ideal case for exploring the structure and function of an enzymatic reaction.

In summary, a pair of site-directed mutations in the active site of isocitrate dehydrogenase has been studied by steady state kinetics and X-ray crystallographic analysis. On the basis of our observations, the most straightforward model for the effect of these mutations is that the removal of a specific chemical group (a hydroxyl from tyrosine 160 or a primary amine nitrogen from lysine 230) causes a reduction in the rate of specific steps in the chemical mechanism of dehydrogenation and decarboxylation, primarily through the loss of an important chemical group in the active site rather than because of changes in tertiary structure which might alter substrate binding or overall mechanism. The argument that mutation of tyrosine 160 and lysine 230 causes no significant mechanistic effects other than deletion or substitution of specific atoms in the active site is based on three observations: the apoenzyme of each mutant exhibits the same fold and conformation as wild-type enzyme, the substrate (an isocitrate/magnesium chelate) is bound by each mutant in a complex that is isomorphous to wild-type enzyme, and both enzyme mutants display an individual rate constant within the overall turnover mechanism which is relatively unchanged from wild-type enzyme (Y160F catalyzes the decarboxylation step at a normal rate; K230M catalyzes the formation of isocitrate from oxalosuccinate at a rate reduced by one-third that of wild-type enzyme) while exhibiting a severe reduction in the rate of an adjacent catalytic step which can be easily ascribed to the effect of the specific mutation.

However, such an interpretation might overlook other important explanations for the observed reduction in rates. Specifically, the structural analyses presented here (of the uncomplexed enzyme and the binary complex with isocitrate and magnesium) do not present data about the binding of the $NADP^+$ cofactor or about conformational transitions which may occur during formation of the productive ternary Michaelis complex and subsequent turnover. It is possible that the small structural changes in structures described above, due solely to the site-directed mutations, may perturb the energetics of a catalytically important conformational change necessary for transition state stabilization and therefore be responsible for the observed decrease of specific rate constants. NAD/NADP-requiring dehydrogenases frequently undergo conformational transitions between open and closed forms during the catalytic cycle, implying that the binary complexes undergo further change to become catalytically active structures. However, examination of the binding of $NADP^+$ cofactor (Hurley *et al.*, 1991) and of the ternary complex formed by the enzyme (Stoddard *et al.*, 1993) indicates that the mutated residues are not involved in nicotinamide binding; likewise, the enzyme does not undergo any significant conformational rearrangements during formation of the initial productive ternary Michaelis complex which these mutations would be likely to affect at a specific catalytic step.

A second consideration with respect to the effect of possible structural changes caused by the mutations discussed above is the possibility that the changes in activity reflect larger perturbations of the protein conformation in solution that those observed crystallographically. In this case, the packing relationships in the crystal could be envisioned to keep the mutant side chains in the same relative conformations and positions as in the wild-type counterpart, whereas in solution these mutated side chains might differ significantly in structure and therefore account for the change in activity. However, the estimated energetic contribution of crystal lattice contacts are usually far smaller than the energetic cost of reorganizing the interactions which stabilize side chain conformations of partially buried side chains in solution, making such a crystallization-driven structural rearrangement unlikely. Examination of the mutated side chains and their immediate neighbors within the packing of the unit cell shows that they do not participate in any crystal contacts, implying that the reported structures are indicative of the actual structural changes in solution.

REFERENCES

Atkinson, & Koshland, D. E., Jr. (1977) *Academy Press.*

Bernstein, F. C., Koetzle, T. F., Williams, G. J. B., Meyer, E. F., Jr., Brice, M. D., Rodgers, J. R., Kennard, O., Shimanouchi, T., & Tasumi, M. (1977) *J. Mol. Biol. 112*, 535−542.

Brunger, A. T., Kuriyan, J., & Karplus, M. (1987) *Science 235*, 458.

Cleland, W. W. (1982) *Methods Enzymol. 87*, 390−405.

Cupp, J. R., & McAlister-Henn, L. (1991) *J. Biol. Chem. 267*, 16417−16423.

Dean, A. M., & Koshland, D. E., Jr. (1990) *Science 249*, 1044−1046.

Dean, A. M., Lee, M. H. I., & Koshland, D. E., Jr. (1989) *J. Biol. Chem. 264*, 20482−20486.

Dente, L., Cesareni, G., & Cortese, R. (1983) *Nucleic Acids Res. 11*, 1645−1655.

Erlich, R. S., & Colman, R. F. (1987) *Biochemistry 26*, 3461−3466.
Fersht, A. R., Shi, J. P., Knill-Jones, J., & Lowe, D. M. (1985) *Nature 314*, 235−238.
Garnak, M., & Reeves, H. C. (1979) *Science 203*, 1111−1112.
Grissom, C. B., & Cleland, W. W. (1988) *Biochemistry 27*, 2934−2943.
Hasselbeck, R. J., & McAlister-Henn, L. (1991a) *J. Biol. Chem. 266*, 2339−2345.
Hasselbeck, R. J., & McAlister-Henn, L. (1991b) *J. Biol. Chem. 266*, 22199−22205.
Hasselbeck, R. J., Colman, R. F., & McAlister-Henn, L. (1992) *Biochemistry 31*, 6219−6223.
Hurley, J., Thorsness, P. E., Ramalingam, V., Helmers, N. H., Koshland, D. E., Jr., & Stroud, R. M. (1989) *Proc. Natl. Acad. Sci. U.S.A. 86*, 8635−8639.
Hurley, J., Dean, A. M., Thorsness, P. E., Koshland, D. E., Jr., & Stroud, R. M. (1990a) *J. Biol. Chem. 265*, 3599−3502.
Hurley, J., Dean, A. M., Sohl, J. L., Koshland, D. E., Jr., & Stroud, R. M. (1990b) *Science 249*, 1012−1016.
Hurley, J., Dean, A. M., Koshland, D. E., Jr., & Stroud, R. M. (1991) *Biochemistry 30*, 8671−8678.
Imada, K., Sato, M., Tanaka, N., Katsube, Y., Maysuura, Y., & Oshima, T. (1991) *J. Mol. Biol. 222*, 725−738.
Jones, T. A. (1978) *J. Appl. Crystallogr. 11*, 268−272.
Kunkel, T. A. (1985) *Proc. Natl. Acad. Sci. U.S.A. 82*, 488−492.
Lienhard, G. E., LaPorte, D., Rose, I. A., & Koshland, D. E., Jr. (1964) *Biochemistry 3*, 185−190.
Migazaki, K., & Oshima, T. (1993) *FEBS Lett. 332*, 37−38.
Ochoa, S. (1948) *J. Biol. Chem. 174*, 115−122.
Steyaert, J., Hallenger, K., Wyns, L., & Stanssens, P. (1990) *Biochemistry 29*, 9064−9072.
Stoddard, B. L., & Koshland, D. E., Jr. (1993) *Biochemistry 32*, 9317−9322.
Stoddard, B. L., Dean, A., & Koshland, D. E., Jr. (1993) *Biochemistry 32*, 9310−9316.
Thomas, P. G., Russell, A. J., & Fersht, A. R. (1985) *Nature 318*, 375−376.
Yang, Y., & Wells, W. W. (1991) *J. Biol. Chem. 266*, 12759−12765.

BI9416115